Preprints of the 19th World Congress
The International Federation of Automatic Control
Cape Town, South Africa. August 24-29, 2014

A Novel Method for Modelling Cellular Response Genome Stress by Combined Gene-Environment Network (GEN) and Kinetic Theory Framework

Jin-Peng. Qi*[#], Qing. Zhang[#], and Jie. Qi*

** College of Information Science & Technology, Donghua University, Shanghai, P.R. China 201620*
(Tel: 86-21-67792314; e-mail: qipengkai@dhu.edu.cn, jieqi@dhu.edu.cn)
[#] The Australia E-Health Research, CSIRO, Brisbane, QLD 4029, Australia
(e-mail: qing.zhang@csiro.au)

Abstract: Under acute Ion Radiation (IR) perturbation from external environment, a normal cell can trigger a series of cellular self-defensive mechanisms. To model the complicated Cellular Response Genome Stress (CRGS, for short), a novel method is proposed based on combined Gene-Environment Network (GEN) and Kinetic Theory of Active Particle (KTAP) framework. In this method, the integrated CRGS model is divided into three subsystems, and each subsystem is composed of different particles with different discrete states at molecular level. Then the dynamic kinetics of integrated CRGS is dealt as outcomes of complicated mutual interactions among molecular particles from different subsystems and external environment cofactors at systematic level. The simulation results show that our method is efficient to illustrate a series of cellular activities, including stochastic Double Strand Break (DSB) generation and repair, switch-like Ataxia Telangiectasia Mutated (ATM) activation, oscillating P53-MDM2 feedback loop as well, and helpful to analyze the capability of cellular self-defensive mechanism, as well as genome stability in response to different IR perturbation circumstances.

1. INTRODUCTION

As one unit of bio-system, a cell, consists of a large number of active molecules, such as, DNA, mRNA, protein etc (Bellouquid and Delitala 2006; Bellouquid and Delitala 2006). Under acute perturbation from outer environment, a cell can start a series of inner activities in response to genome stress (Perez and Brady 1999; Li, Story et al. 2001). For example, under acute IR, Double Strand Breaks (DSBs) occur in a normal cell stochastically. Fortunately, a cell can fix these DNA damage by cellular self-repair mechanisms, and then keep genome stability. To investigate the complicated mechanisms of biological system, currently, the combined approaches of control theory, system biology and bioinformatics can stimulate new ideas, which provide a good link between diverging areas of biomedicine and mathematics (Chou 2004; Bellomo, Bellouquid et al. 2010). Recently, several existing methods are used to represent the complicated cellular activities in response to genome stress via P53 signal pathway models. For example, the stochastic models of p53 system were proposed in (Puszyński, Hat et al. 2008; Cai and Yuan 2009; Leenders and Tuszynski 2013). Also, other models of p53 were investigated, such as in (Batchelor, Loewer et al. 2011), (Kim, Rho et al. 2009), (Qi, Shao et al. 2007; Qi, Shao et al. 2008; Qi, Ding et al. 2009; Zhang, Liu et al. 2012), and (Ma, Wagner et al. 2005).

On the other hand, as a novel mathematical framework, KTAP can be used in modelling the overall system by evolution equations corresponding to the dynamics of all their elements (Bellomo and Delitala 2008; Brazzoli 2008). In terms of KTAP framework, a biological phenomenon can be dealt as an evolution of dynamics of several interacting modules (Bellouquid and Delitala 2006; Bellomo and Forni 2008), and the description of bio-system essentially means defining microscopic state of these interacting molecules and distribution function under the state above (Bellouquid and Delitala 2006). KTAP is motivated not only by applied mathematicians, but also by researchers in the field of biological science. The methodology of statistical mechanics and kinetic theory to model complex biological system is capturing the attention of more and more applied mathematicians (Degond, Pareschi et al. 2004; Brazzoli 2008; Yu, Wacholder et al. 2012). Moreover, KTAP is applied in various fields of social and life science, e.g. modelling social behaviour of interacting individuals (Bertotti and Delitala 2008), especially, multi-cellular systems (Bellouquid and Delitala 2006; Bellomo and Forni 2008; Bellomo, Bellouquid et al. 2010), tumour-immune system competition (Bellomo and Forni 2008), as well as cellular self-repair mechanisms (Qi, Ding et al. 2011).

To investigate a series of cellular self-defensive activities in response to acute IR perturbation from outer environment, in this paper, a novel method is proposed to model CRGS based on the combined GEN and KTAP framework. In this method, the integrated CRGS model is divided into three subsystem, including the stochastic DSB generation and repair, switch-like ATM activation, oscillating P53-MDM2 feedback loop as well. Each part is composed of the different molecular particles with different discrete states, and then the dynamic kinetics of the integrated CRGS is dealt as the consequences

of complicated mutual interactions among molecular particles within different subsystems and external environment cofactors. Comparing with the deterministic ODE methods, our method can well not only describe stochastic mutual interactions among large-scale active particles at molecule level, but also demonstrate the complicated and dynamic kinetics of cellular self-defensive activities in response to external environment perturbation cofactors at system level. In the following paragraphs, Section.2 gives the proposed method in detail, including a brief survey of CRGS model, and the detailed implementation of CRGS model. Section.3 simulates the dynamic kinetics of integrated CRGS model, and roughly analyzes cellular self-defensive capability and genome stability under different IR perturbations. Section.4 gives the conclusion of above research.

2. METHOD

2.1 Survey of CRGS model

Based on the combined GEN and KTAP framework, our CRGS model aims to investigate cellular self-defensive mechanisms in response to genome stress at molecule and single cell levels. Fig.1 is the profile of CRGS model under acute IR perturbation. It is composed of three subsystems: DBS generation and repair, ATM activation, and P53-MDM2 feedback loop. Each subsystem includes active particles with different microscopic active states. Moreover, acute IR and molecular interactions may modify either the state of each molecular or the number of molecular in each population by proliferation/destruction phenomena (Bellouquid and Delitala 2006; Bellouquid and Delitala 2006; Brazzoli 2008).

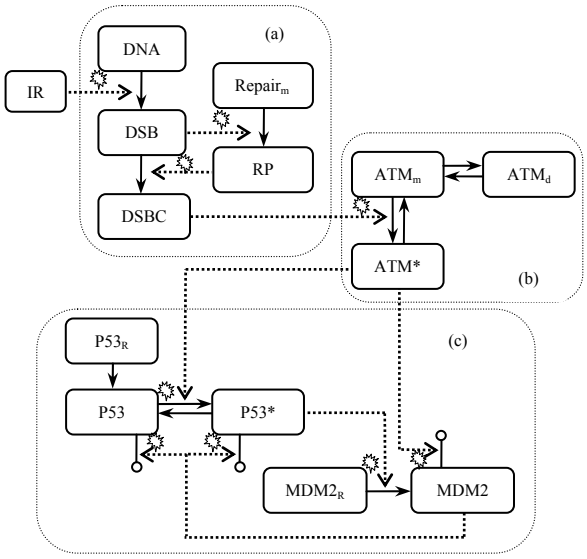

Fig.1. The diagram of CRGS model under IR perturbation. It is composed of three subsystems, including (a) DBS generation and repair, (b) ATM activation, and (c) P53-MDM2 feedback loop. (Arrow-headed solid lines refer to state transition, and arrow-headed dotted lines stand for promotion of state transition, respectively. Bombing icons indicate the mutual interactions between two active molecular particles.)

As acute IR is applied to a cell, the first part represents the stochastic kinetics of DSB generation and repair processes. The second part denotes switch-like ATM activation under DSBC signal transferring; and the third part illustrates the oscillating kinetics of P53-MDM2 feedback loop induced by ATM activation, which is essential to trigger cellular response in fighting against genome stress further (Oren 2003; Ma, Wagner et al. 2005). To simplify the model, we assume the active particles in different subsystems are homogeneously distributed in space, undergoing localized binary interactions, in which the test particle enters into the action domain of the field particle (Brazzoli 2008). Due to the complicated mechanisms in CRGS, the integrated model above is just a simple description and simulation for the complicated cellular self-defensive activities. The limited vital genes and environment cofactors, as well as their mutual interactions and regulating pathways are involved into our integrated model.

2.2 Implementation of CRGS model

The dynamic kinetics of integrated CRGS model is composed of three parts, including stochastic DSB generation and repair, switch-like ATM activation, as well as oscillating P53-MDM2 feedback loop, respectively. In the following paragraphs, f_x denotes the normalized concentration density of the molecular particle x. S_x is the basal generation rate of particle x from its initial state. $\eta_{x\circ y}$ stands for the encounter rate of molecular particle x with particle y. $B_{x\to x'}^{x\circ y}$ refers to the probability of a particle x transforming into the state x' from initial state under mutual interaction with particle y. $K_{x\to x'}$ refers to the probability of a molecular x transforming into state x' from its initial state without any interference. d_x is the degradation rate of molecule particle x.

In the **DSB generation and repair sub-system** shown in Fig.1.(a), DNA in a cell is broken down in response to external IR perturbation, and then DSBs occur stochastically. For a normal cell, it can fix DNA damage through self-repair mechanisms (Rothkamm, Krüger et al. 2003). In this period, Repair Protein (RP), a repair enzyme, can bind into the nascent DNA end and synthesize DSB-protein complex (DSBC) (Budman and Chu 2005). As a main signal source to transfer genome damage, DSBC can relay DNA damage to downstream ATM gene, and then trigger switch-like kinetics of ATM activation (Kohn and Pommier 2005). Under mutual interaction between repair gene (the test particle) and DSB (the field particle), repair mRNA transcription is prompted, and then RP translation is accelerated by mutual interaction between repair mRNA and DSB. Providing that RP is available around DNA damage site, DSBC synthesis is promoted by mutual interactions of DSB with RP (Qi, Ding et al. 2011). The correct repair part of DSBCs (rDSBCs) is dealt as a main signal to transfer damage signal to downstream genes and regulation pathways. Whereas, the disrepair part of DSBCs (mDSBCs) and intact DSBs will be remained in a cell, which can seriously weaken genome stability and cellular viability, even lead to abnormal and cancerous eventually (Ma, Wagner et al. 2005). The

stochastic kinetics of DSB generation and repair can be represented by the following equations:

$$\frac{df_{DSB}}{dt} = C_i \cdot C^{e}_{DNA\circ IR} \cdot B^{DNA\circ IR}_{DNA\to DSB} \cdot g^{(p)}_{IR} \cdot f_{DNA}\,, \quad (1)$$

$$B^{DNA\circ IR}_{DNA\to DSB} = K_{DSB\circ t} \cdot Poissrnd\left(a_{IR} \cdot g^{(P)}_{IR}\right), \quad (2)$$

$$\frac{df_{repairR}}{dt} = S_{repairR} \cdot f_{repairG} + \eta_{repairG\circ DSB} \cdot B^{repairG\circ DSB}_{repairG\to repairR} \cdot f_{repairG} \cdot f_{DSB} - \eta_{repairR\circ DSB} \cdot B^{repairR\circ DSB}_{repairR\to RP} \cdot f_{repairR} \cdot f_{DSB} - d_{repairR} \cdot f_{repairR}\,, \quad (3)$$

$$\frac{df_{RP}}{dt} = S_{RP} \cdot f_{repairR} + \eta_{repairR\circ DSB} \cdot B^{repairR\circ DSB}_{repairR\to RP} \cdot f_{repairR} \cdot f_{DSB} - d_{RP} \cdot f_{RP} \quad (4)$$

$$\frac{df_{rDSBC}}{dt} = \eta_{DSB\circ RP} \cdot B^{DSB\circ RP}_{DSB\to rDSBC} \cdot f_{RP} \cdot f_{DSB} - K_{rDSBC\to DSB} \cdot f_{rDSBC}\,, \quad (5)$$

$$\frac{df_{mDSBC}}{dt} = \eta_{DSB\circ RP} \cdot B^{DSB\circ RP}_{DSB\to mDSBC} \cdot f_{RP} \cdot f_{DSB} - K_{mDSBC\to DSB} \cdot f_{mDSBC}\,, \quad (6)$$

$$f_{RDSB} = f_{DSB} - f_{rDSBC} - f_{mDSBC}\,,\ f_{toxins} = f_{RDSB} + f_{mDSBC}\,, \quad (7)$$

where C_i refers the rate of DNA damage generation in accordance with different cell types. $C^{e}_{DNA\circ IR}$ is the encounter rate of DNA and external IR perturbation cofactor. $K_{DSB\circ t}$ is the number of DSBs generation within each time scale, and a_{IR} is the number of DSBs generation induced by per IR dose.

In the **ATM activation sub-system** shown in Fig.1.(b), ATM, a detector of DNA damage, is extremely sensitive to genome stress induced by external perturbation (Bakkenist and Kastan 2003; Pauklin, Kristjuhan et al. 2005). In response to damage signal transferred from DSBC synthesis, inactive ATM dimmer is phosphorylated into active ATM (ATM*) after positive interaction with rDSBC particles. Generally, ATM activation is a reversible kinetics, that is, ATM monomer can convert into ATM dimmer, and active ATM (ATM*) can transform into ATM dimmer reversibly. In addition, the total concentration of ATM including ATM dimmer, ATM monomer and ATM* is supposed to be a constant in the cell (Ma, Wagner et al. 2005; Qi, Ding et al. 2011). The kinetics of ATM activation is represented by following formulas:

$$\frac{df_{ATMd}}{dt} = \frac{1}{2} K_{ATMm\to ATMd} \cdot f^{2}_{ATMm} - K_{ATMd\to ATMm} \cdot f_{ATMd}\,, \quad (8)$$

$$\frac{df_{ATMm}}{dt} = 2K_{ATMd\to ATMm} \cdot f_{ATMd} - K_{ATMm\to ATMd} \cdot f^{2}_{ATMm} - \eta_{ATMm\circ rDSBC} \cdot B^{ATMm\circ rDSBC}_{ATMm\to ATM^*} \cdot f_{ATMm} \cdot f_{rDSBC} + K_{ATM^*\to ATMm} \cdot f_{ATM^*}\,, \quad (9)$$

$$\frac{df_{ATM^*}}{dt} = \eta_{ATMm\circ rDSBC} \cdot B^{ATMm\circ rDSBC}_{ATMm\to ATM^*} \cdot f_{ATMm} \cdot f_{rDSBC} - K_{ATM^*\to ATMm} \cdot f_{ATM^*} \quad (10)$$

In the **P53-MDM2 feedback loop sub-system** plotted in Fig.1. (c), P53-MDM2 feedback loop is kernel in P53 network, whose function is to cease cell propagation and in certain cases cause apoptosis (Vogelstein, Lane et al. 2000; Oren 2003; Meek 2004; Ma, Wagner et al. 2005; Pauklin, Kristjuhan et al. 2005). In response to signal transferring from ATM activation, P53 phosphorylation is prompted by positive interaction with ATM* molecular (Vogelstein, Lane et al. 2000; Pauklin, Kristjuhan et al. 2005). Meanwhile, MDM2 degradation is accelerated by negative interaction with ATM* molecular. On the other hand, the expression of MDM2 is accelerated under positive interaction with P53* particles. Whereas, the concentration of P53* is depressed by negative interaction with MDM2, a P53-specific ligase and antagonist of P53 (Ma, Wagner et al. 2005), in order to keep dynamic equilibrium of P53-MDM2 feedback loop, and avoid the over-expression of P53. Once the dynamic equilibrium of 53-MDM2 feedback loop is broken, as a result, the expected dynamic oscillation will occur between P53 and MDM2 (Ma, Wagner et al. 2005; Qi, Ding et al. 2011). The main formulations used in this module are as follows:

$$\frac{df_{P53}}{dt} = S_{P53} \cdot f_{P53R} + K_{P53^*\to P53} \cdot f_{P53^*} - \eta_{P53\circ ATM^*} \cdot B^{P53\circ ATM^*}_{P53\to P53^*} \cdot f_{ATM^*} \cdot f_{P53} - \eta_{P53\circ MDM2} \cdot B^{P53\circ MDM2}_{P53\to \deg P53} \cdot f_{MDM2} \cdot f_{P53} - d_{P53} \cdot f_{P53}\,, \quad (11)$$

$$\frac{df_{P53^*}}{dt} = \eta_{P53\circ ATM^*} \cdot B^{P53\circ ATM^*}_{P53\to P53^*} \cdot f_{ATM^*} \cdot f_{P53} - K_{P53^*\to P53} \cdot f_{P53^*} \eta_{P53^*\circ MDM2} \cdot B^{P53^*\circ MDM2}_{P53^*\to \deg P53^*} \cdot f_{MDM2} \cdot f_{P53^*} - d_{P53^*} \cdot f_{P53^*}\,, \quad (12)$$

$$\frac{df_{MDM2R}}{dt} = S_{MDM2R} - \eta_{MDM2R\circ P53^*} \cdot B^{MDM2R\circ P53^*}_{MDM2R\to MDM2} \cdot f_{MDM2R} \cdot f_{P53^*} - d_{MDM2R} \cdot f_{MDM2R}\,, \quad (13)$$

$$\frac{df_{MDM2}}{dt} = S_{MDM2} \cdot f_{MDM2R} + \eta_{MDM2R\circ P53^*} B^{MDM2R\circ P53^*}_{MDM2R\to MDM2} \cdot f_{MDM2R} \cdot f_{P53^*} - \eta_{MDM2\circ ATM^*} \cdot B^{MDM2\circ ATM^*}_{MDM2\to \deg MDM2} \cdot f_{ATM^*} \cdot f_{MDM2} - d_{MDM2} \cdot f_{MDM2}\,, \quad (14)$$

The other related equations used in the integrated CRGS model can be found in Appendix A in detail.

3. RESULT AND DISCUSSION

By using platform of Matlab.7, the dynamics of CRGS are illustrated under different IR perturbation circumstances. In our simulations, the different 1, 5, 10, and 15Gy IR dose are applied into a normal cell, respectively. The concentrations of active molecule particles are denoted by the marks [*] in all figures of simulation results. The dimensionless parameters are shown in Appendix B in detail, which are taken and revised from (Ma, Wagner et al. 2005; Qi, Ding et al. 2009; Qi, Ding et al. 2011; Zhang, Liu et al. 2012).

3.1 Stochastic kinetics of DSB generation and repair

As shown in Fig.2, in response to external interaction with acute IR perturbation cofactors from outer environment,

different numbers of resulting DSBs occur stochastically, and the more DSBs are generated as the stronger IR is applied. As a result, RP is translated from repair mRNA under mutual interaction with resulting DSBs, and the more resulting DSBs induced by stronger IR, the less RP is available around damage site. Thereafter, resulting DSBs are synthesized into DSBC under mutual interaction with RP available, and fewer numbers of rDSBCs are synthesized as available RPs decrease against stronger IR Perturbation cofactor. These simulations show that RP available can be dealt as an indicator of cellular self-repair capability in a normal cell. Whereas, this capability begins to decrease as the strength of external perturbation cofactor overtakes the threshold that a normal cell can burden maximally.

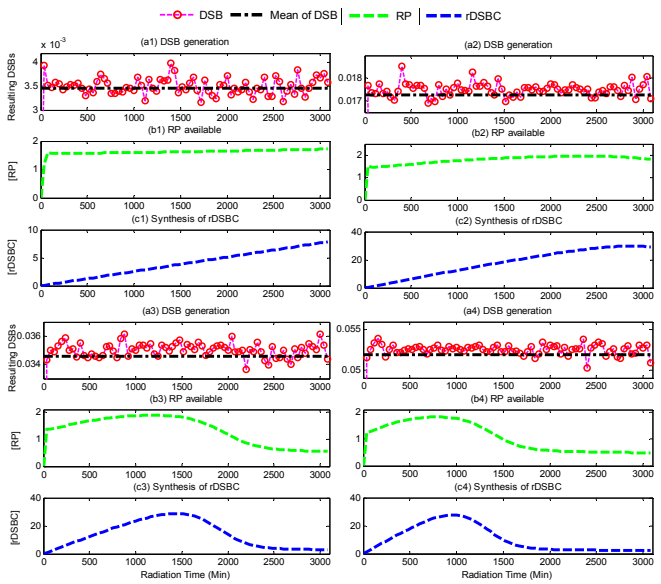

Fig.2. The stochastic kinetics of DSB generation and repair in response to external IR perturbation cofactors. (a1-a4) stochastic trace of DSB generation; (b1-b4) RP available around damage sites; and (c1-c4) rDSBC synthesis under 1,5,10, and 15Gy IR, respectively.

3.2 Oscillations of P53-MDM2 under ATM activation

As a detector of genome stress, ATM is very sensitive to damage signal from DSBC synthesis. In response to mutual interaction with rDSBC molecular, ATM is activated from inactive ATM monomer (ATMm), as f_{rDSBC} overtake the minimal threshold that ATM can sense. As shown in Fig.3, in response to different IR perturbations, the switch-like ATM activation occur after a period of radiation time scales, and the stronger IR is applied, the shorter time is needed. After activated, the phosphorylated ATM (ATM*) rapidly rises to a high plateau and keeps dynamic equilibrium until f_{rDSBC} is below the minimal threshold. The shorter duration that ATM activation can keep when the stronger IR is applied, because limited RPs are available around increasing damage sites, and f_{rDSBC} is lower that ATM cannot be detected. Then, the dynamic equilibrium of P53-MDM2 feedback loop is broken, as a result, oscillations occur between P53 and MDM2, after mutual interaction with ATM* particles.

The dynamic oscillations between P53 and MDM2 keep active similarly with ATM activation, and the period of oscillation is shorter as stronger IR is applied. To some extent, these results are quite similar to the experimental observations and in accordance with existing studies in (Ma *et al*., 2005; Qi *et al*., 2008; 2009). The simulations above indicate that switch-like ATM activation can relay genome stress signal induced by external perturbation cofactors, and then transfer to P53-MDM2 feedback loop further. In addition, the periodical oscillations between P53 and MDM2 suggest that once self-defensive mechanisms is triggered, a series of cellular activities can be started, e.g., cell cycle arrest, and cell apoptosis etc.

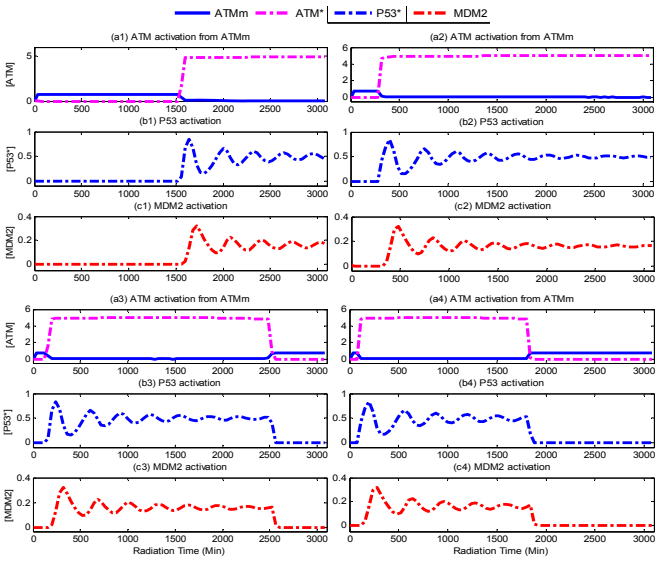

Fig.3. The oscillations of P53-MDM2 feedback loop in response to switch-like ATM activation. (a1-a4) Switch-like ATM activation; (b1-b4) oscillations of P53 activation; and (c1-c4) oscillations of MDM2 activation, under 1, 5, 10, and 15Gy IR perturbation, respectively.

3.3 Genome stability analysis

Although a normal cell can defence external perturbations properly through a series of cellular activities, some inevitable toxins, such as, intact DSBs and mDSBC might be accumulated in a cell, which damage cellular response capability and genome stability, even lead to fatal cancer (Qi *et al*., 2011; Ma *et al*., 2005). Therefore, we propose that a number of toxins remained in a cell can decrease genome stability directly. In our simulations, Fig.4 shows that f_{mDSBC}, a by-product of DSBs repair process, is fluctuated in accordance with RP available and rDSBC synthesis shown in Fig.2. On the other hand, as another part of toxin, intact DSBs keep increasing against radiation time, and the remained DSBs increase faster, especially when stronger IR is applied, because of the limited RP available around increasing damage cites. As a result, genome stability keeps decreasing against toxin accumulating in response to different IR perturbations, and the more strength of IR is applied, the more damage for genome stability occurs. These results suggest that, a normal cell can deal with genome stress efficiently by means of a series cellular self-defensive activities, whereas, cellular self-repair capability, and genome stability might be damaged, even lethal cancerous or apoptosis occur as the strength of external perturbation

overwhelms the threshold that a normal cell can burden maximally.

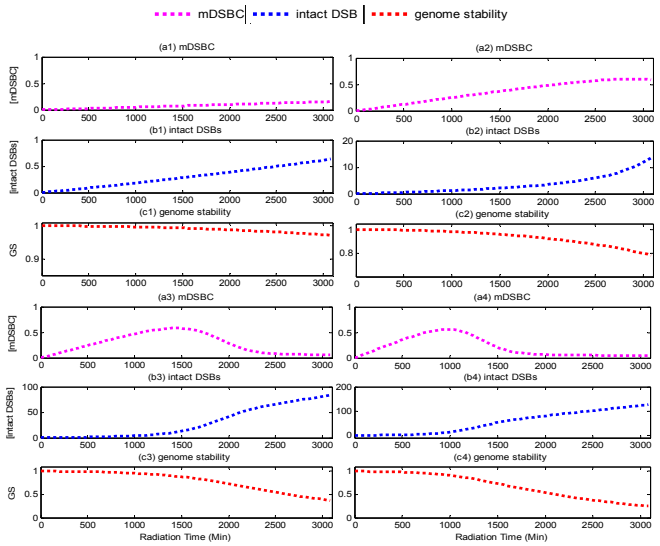

Fig.4. Analysis for genome stability in response to toxin accumulation under different IR perturbations. (a1-a4) The kinetics of mDSBC generation; (b1-b4) intact DSBs accumulation; as a result, (c1-c4) genome stability decreasing, under 1, 5, 10, and 15Gy IR, respectively.

4. CONCLUSION

Based on GEN and KTAP framework, an integrated model of CRGS is proposed to represent a series of cellular activities in response to genome stress under external IR perturbation. In this work, CRGS model is divided into three subsystems. Each subsystem is composed of different molecular particles with different discrete states. The systematic kinetics of cellular response activities are dealt as results of the complicated mutual interactions among different particles from different subsystems. The simulations show that our method can successfully illustrate the dynamics of CRGS, including stochastic DSB generation and repair, switch-like ATM activation, and oscillations of P53-MDM2 feedback loop, and analyze cellular self-defensive capability, as well as genome stability in response to genome stress under different IR perturbation circumstances. The proposed method is flexible and efficient in capturing stochastic interactions in cellular activities at molecular level, as well as dynamic evolution of CRGS at systematic level; especially, it is very helpful to deeply investigate and analyze the complicated cellular self-defending mechanisms in response to acute perturbation cofactors from outer environment.

ACKNOWLEDGMENT

I would like to thank my supervisor Prof. Qing. Zhang in the Australia e-Health Research Centre for his assistance, support and advice for this paper. This paper is supported by National Natural Science Foundation of China (No.61104154), and the Fundamental Research Funds for the Central Universities.

REFERENCES

Bakkenist, C. J. and M. B. Kastan (2003). "DNA damage activates ATM through intermolecular autophosphorylation and dimer dissociation." Nature **421**(6922): 499-506.

Batchelor, E., A. Loewer, et al. (2011). "Stimulus‐dependent dynamics of p53 in single cells." Molecular systems biology **7**(1).

Bellomo, N., A. Bellouquid, et al. (2010). "Complexity and mathematical tools toward the modelling of multicellular growing systems." Mathematical and Computer Modelling **51**(5): 441-451.

Bellomo, N. and M. Delitala (2008). "From the mathematical kinetic, and stochastic game theory to modelling mutations, onset, progression and immune competition of cancer cells." Physics of Life Reviews **5**(4): 183-206.

Bellomo, N. and G. Forni (2008). "Complex multicellular systems and immune competition: New paradigms looking for a mathematical theory." Current Topics in Developmental Biology **81**: 485-502.

Bellouquid, A. and M. Delitala (2006). Mathematical modeling of complex biological systems: a kinetic theory approach, Springer.

Bellouquid, A. and M. Delitala (2006). "Modelling Complex Multicellular Systems-A Kinetic Theory Approach." Birkäuser, Boston.

Bertotti, M. L. and M. Delitala (2008). "Conservation laws and asymptotic behavior of a model of social dynamics." Nonlinear Analysis: Real World Applications **9**(1): 183-196.

Brazzoli, I. (2008). "From the discrete kinetic theory to modelling open systems of active particles." Applied Mathematics Letters **21**(2): 155-160.

Budman, J. and G. Chu (2005). "Processing of DNA for nonhomologous end‐joining by cell‐free extract." The EMBO journal **24**(4): 849-860.

Cai, X. and Z.-M. Yuan (2009). "Stochastic modeling and simulation of the p53-MDM2/MDMX loop." Journal of Computational Biology **16**(7): 917-933.

Chou, K.-C. (2004). "Structural bioinformatics and its impact to biomedical science." Current medicinal chemistry **11**(16): 2105-2134.

Degond, P., L. Pareschi, et al. (2004). Modeling and computational methods for kinetic equations, Springer.

Kim, D.-H., K. Rho, et al. (2009). "A theoretical model for p53 dynamics Identifying optimal therapeutic strategy for its activation and." Cell Cycle **8**(22): 3707-3716.

Kohn, K. W. and Y. Pommier (2005). "Molecular interaction map of the p53 and Mdm2 logic elements, which control the Off–On switch of p53 in response to DNA damage." Biochemical and biophysical research communications **331**(3): 816-827.

Leenders, G. B. and J. A. Tuszynski (2013). "Stochastic and deterministic models of cellular p53 regulation." Frontiers in oncology **3**.

Li, L., M. Story, et al. (2001). "Cellular responses to ionizing radiation damage." International Journal of Radiation Oncology* Biology* Physics **49**(4): 1157-1162.

Ma, L., J. Wagner, et al. (2005). "A plausible model for the digital response of p53 to DNA damage." Proceedings of the National Academy of Sciences of the United States of America **102**(40): 14266-14271.

Meek, D. W. (2004). "The p53 response to DNA damage." DNA repair **3**(8): 1049-1056.

Oren, M. (2003). "Decision making by p53: life, death and cancer." Cell Death & Differentiation **10**(4): 431-442.

Pauklin, S., A. Kristjuhan, et al. (2005). "ARF and ATM/ATR cooperate in p53-mediated apoptosis upon oncogenic stress."

Biochemical and biophysical research communications **334**(2): 386-394.

Perez, C. and L. Brady (1999). "Principles and practice of radiation oncology." Journal of Pediatric Hematology/Oncology **21**(6): 560.

Puszyński, K., B. Hat, et al. (2008). "Oscillations and bistability in the stochastic model of p53 regulation." Journal of Theoretical Biology **254**(2): 452-465.

Qi, J.-P., S.-H. Shao, et al. (2007). "A dynamic model for the p53 stress response networks under ion radiation." Amino Acids **33**(1): 75-83.

Qi, J., Y. Ding, et al. (2009). "Dynamic modeling of cellular response to DNA damage based on p53 stress response networks." Progress in Natural Science **19**(10): 1349-1356.

Qi, J., Y. Ding, et al. (2011). "Kinetic theory approach to modeling of cellular repair mechanisms under genome stress." PloS one **6**(8): e22228.

Qi, J., S. Shao, et al. (2008). "Cellular responding DNA damage: An improved modeling of P53 gene regulatory networks under ion radiation (IR)." Applied Mathematics and Computation **205**(1): 73-83.

Rothkamm, K., I. Krüger, et al. (2003). "Pathways of DNA double-strand break repair during the mammalian cell cycle." Molecular and cellular biology **23**(16): 5706-5715.

Vogelstein, B., D. Lane, et al. (2000). "Surfing the p53 network." Nature **408**(6810): 307-310.

Yu, K., S. Wacholder, et al. (2012). "A Flexible Bayesian Model for Studying Gene–Environment Interaction." PLoS genetics **8**(1): e1002482.

Zhang, X.-P., F. Liu, et al. (2012). "Regulation of the DNA damage response by p53 cofactors." Biophysical journal **102**(10): 2251-2260.

Appendix A.

The other related equations used in the integrated CRGS model are as follows:

$$\eta_{repairG\circ DSB}=\frac{f_{DSB}}{f_{DSB}+f_{repairG}}\ ,\ B^{repairG\circ DSB}_{repairG\to repairR}=\frac{k_{SrepairR}\cdot f_{repairR}\cdot f_{P21}}{f_{DSB}+f_{repairG}}\ , \quad (1)$$

$$\eta_{repairR\circ DSB}=\frac{f_{DSB}}{f_{DSB}+f_{repairR}}\ ,\ B^{repairR\circ DSB}_{repairR\to RP}=\frac{k_{SRP}\cdot f_{RP}\cdot f_{P21}}{f_{DSB}+f_{repairR}}\ , \quad (2)$$

$$\eta_{DSB\circ RP}=\frac{f_{RP}}{f_{DSB}+f_{RP}}\ ,\ B^{DSB\circ RP}_{DSB\to rDSBC/mDSBC}=\frac{k_{SrDSBC/SmDSBC}\cdot f_{rDSBC/mDSBC}}{f_{DSB}+f_{RP}}\ , \quad (3)$$

$$\eta_{ATMm\circ rDSBC}=\frac{f_{rDSBC}}{f_{rDSBC}+f_{ATMm}}\ ,\ B^{ATMm\circ rDSBC}_{ATMm\to ATM^*}=\frac{K_{SATM}\cdot f_{ATMm}}{(f_{ATMm}+J_{rDSBC\to ATM^*})}\ , \quad (4)$$

$$K_{ATM^*\to ATMm}=\frac{K_{deATM}\cdot f_{ATM^*}}{(f_{ATM^*}+J_{ATM^*\to ATMm})}\ , \quad (5)$$

$$\eta_{P53\circ ATM^*}=\frac{f_{ATM^*}}{f_{P53}+f_{ATM^*}}\ ,\ B^{P53\circ ATM^*}_{P53\to P53^*}=\frac{K_{sP53^*}}{f_{P53}+J_{ATM^*\to P53^*}}\ , \quad (6)$$

$$\eta_{P53/P53^*\circ MDM2}=\frac{f_{MDM2}}{f_{P53/P53^*}+f_{MDM2}}\ , \quad (7)$$

$$B^{P53\circ MDM2}_{P53/P53^*\to \deg}=\frac{K_{dP53/P53^*}}{f_{P53}+J_{MDM2\to dP53/P53^*}}\ , \quad (8)$$

$$\eta_{MDM2\circ ATM^*}=\frac{f_{ATM^*}}{f_{ATM^*}+f_{MDM2}}\ , \quad (9)$$

$$B^{MDM2\circ ATM^*}_{MDM2\to \deg MDM2}=\frac{K_{dMDM2}}{f_{ATM^*}+J_{ATM^*\to dMDM2}}\ , \quad (10)$$

$$\eta_{MDM2R\circ P53^*}=\frac{f_{P53^*}}{f_{P53^*}+f_{MDM2R}}\ , \quad (11)$$

$$B^{MDM2R\circ P53^*}_{MDM2R\to MDM2}=\frac{K_{sMDM2}\cdot f_{P53^*}\text{^}4}{f_{P53^*}\text{^}4+J_{P53^*\to MDM2}\text{^}4}\ , \quad (12)$$

where $J_{x\to y}$ is the parameter to set the threshold concentrations for the generation or degradation of the current molecular particles x under interactions with the dependent particle y. K_a in $B^{x\circ y}_{x\to x'}$ stands for the transformation rates of molecular particle a after mutual interacting with another particle within discrete state space.

Appendix B.

Parameter	Value	Parameter	Value
C_i	0.8	S_{P53}	0.15
C^{ε}_{DNA-IR}	1	$K_{P53^*\to P53}$	0.2
$K_{DSB\circ t}$	0.001	d_{P53}	0.02
a_{IR}	35	K_{sP53^*}	0.6
$S_{repairR}$	0.2	K_{dP53}	0.1
$d_{repairR}$	0.1	$J_{MDM2\to dP53}$	0.03
S_{RP}	0.1	K_{dP53^*}	0.01
d_{RP}	0.1	$J_{MDM2\to dP53^*}$	0.03
K_{SrDSBC}	0.99	d_{P53^*}	0.01
K_{SmDSBC}	0.01	S_{MDM2R}	0.1
$K_{rDSBC\to DSB}$	0.1	K_{dMDM2}	0.01
$K_{mDSBC\to DSB}$	0.05	$J_{ATM^*\to dMDM2}$	1.5
$K_{DSB\to DNA}$	1	K_{sMDM2}	0.03
$K_{ATMd\to ATMm}$	1	$J_{P53^*\to MDM2}$	1
$K_{ATMm\to ATMd}$	8	d_{MDM2R}	0.01
K_{SATM}	1.5	d_{MDM2}	0.1
K_{deATM}	0.8		
$J_{rDSBC\to ATM^*}$	1		
$J_{ATM^*\to ATMm}$	2		